Effects of the Blast Vibration Frequency on the Shear Strength of the Joints and Pit Slope Stability

Ali Siamaki, Kamran Esmaeili, Bibhu Mohanty

Lassonde Institute of Mining, University of Toronto, ON, Canada

Blast induced vibrations are the blasting drawbacks which may cause instability in the adjacent and nearby structures. These vibrations could degrade the shear strength of the major discontinuities in the rock mass. Therefore, the bearing capacity of the rock mass may be reduced by the repetitive blasts which lead to the slope instabilities. In this paper, the recorded vibration histories of a single row blast with double deck boreholes in a quarry was considered. The blast histories were recorded at two stations, one on the same bench as the blasting (station S1) and another one on the upper bench (station S2). The results showed peak particle velocities at station S1 were influenced by the upper decks, while the bottom decks have more influence on the recorded peak particle velocities in S2. The dominant wave frequency at station S1 was 121 Hz, while it was 48 Hz at station S2. The recorded vibration loads at each station were applied to a stiff rock block of 2 m height × 1 m width, with a single inclined persistent joint, simulated by 2D Particle Flow Code (PFC2D). The vibration loads, recorded at the two stations, were separately applied to the jointed rock block for consecutive times to model the effect of repeated loading due to separate blasts. The numerical experiments allowed investigation of the interaction between blast-induced stress waves and the joint surface and quantification of the progressive accumulation of damage inflicted along the joint. The vibration-induced damage was equated with the number of micro-cracks generated along the joint surface. The results show that the frequency content has a significant impact on the degradation of joint shear strength in a rock mass. Higher micro-crack generation rate (degradation rate) was recorded along the joint surface when subjected to the lower vibration wave frequency, recorded at station S2. The results show that the numerical method can be used as a diagnostic and predictive tool for characterization of blast-induced damage in open pit mines, when validated by careful blast vibration and slope monitoring programs.

Introduction

Blasting is one of the main activities in mining and construction projects. Although the main purpose of blasting is breaking insitu rock mass into well fragmented rock bolders, a portion of explosive energy is consumed in the form of ground vibration, air shock and flyrock. A good blasting practice should produce appropriate rock fragmentation with acceptable level of ground vibrations according to the standards. In open pit mines, ground vibration caused by repeated blasting can stimulate loose rock blocks in the nearby pit walls, leading eventually to their failure.

Repetitive blasts during the mine life may cause a reduction in the shear strength and bearing capacity of the major discontinuities in the mine site. In addition, it can reduce the rock mass strength as a result of joint degradation within the rock mass. Study of ground vibration effects on discontinuities provides a better understanding of the pit wall and bench stability during their operational life. While many researchers have discussed pit wall instability caused by blasting in the near and far field (Floyd 1998; Yang et al. 2009; Law, 1996; Dianji, 2002; Naismith, 2005; Kong, 2012; O'Bryan, 2012), there is no comprehensive study on joint degradation under repetitive blasting. Only limited investigations have been carried out to analyze and quantify this phenomenon (Mohanty et al., 2017).

In order to understand the response of jointed rock masses to seismic loads in the near field, suitable measurement methods (i.e. high-frequency high-g accelerometers) should be used to study the initiation sequence and the corresponding amplitude and frequency content of blast-

induced vibrations. Accelerometers are capable of recording extremely high vibrations and are very suitable for measuring near the blast holes (Mohanty and Zwaan, 2015).

Measuring joint degradation caused by blasting vibrations in the field is difficult or nearly impossible. Numerical simulation of a simple case based on the recorded vibration history of a production blast in the field reveals how blasting vibration has an effect on joint degradation. Continuum and discontinuum numerical methods have been used to simulate blast-induced damage. These simulations mainly focused on the study of ground vibration propagation within the rock mass, displacement measurement, damage generation and evolution and instabilities in rock mass (Yoon, 2010; Deb, 2011; Onederra, 2012; Hu, 2014; Resende, 2014; Blair, 2015).

Portion of the wave energy is dissipated during wave propagation through discontinuities. Dissipated energy may have impact on the mechanical properties of the joint which leads to the joint degradation. This reduction could result in rock mass degradation. Therefore, stability of rock slopes and wedges in mining environment may decrease by repetitive blasting during the life of the projects.

This paper investigates joint strength degradation under the effects of blast induced vibration. For this purpose, at first, recorded vibration histories of a single row blast on two different benched were examined. Recorded vibration on two benches with different dominant frequencies are used as an input to the developed jointed rock model in PFC2D. Simulation results showed how the joint surface behaves under the incoming ground vibrations from blasting.

Field Instrumentation and Measurement

The recorded ground vibration from a single row blasting in a quarry was taken as the input waveform in this study. The blast row consisted of seven 125 mm diameter double deck holes with the depth of 16 m each. Spacing and burden were 4.0 and 3.6 m, respectively. The initiation system was the shock tube based down hole detonators (500 ms) and there was a 42 ms inter deck delay interval between the upper and bottom decks. The bottom deck was detonated before the upper one in each hole. The blast holes were charged by emulsion explosive (density: 1.25 g/cc) and each deck was initiated with a 454 g Pentolite booster. The charge weight of the bottom decks was approximately 123 kg and the upper one was about 132 kg (except for the last bottom deck, which had only 76 kg in the bottom deck) (Mohanty et al. 2017).

Ground vibration from blasting was measured by two tri-axial accelerometers (Kilster 8702; resonant frequency 54 kHz) grouted into the rock. One of the sensors was on the same bench as the blasting, seismic station S1, and the other one was on the upper bench, seismic station S2. Figure 1 shows locations of the recording stations compared to the blast holes.

Figure 1.

PFC2D only accepts the velocity histories as an input to the model. Therefore, the velocity histories of the recorded components were obtained by numerical integration of the acceleration histories. Figure 2 shows the recorded velocity components at the two monitoring stations.

Figure 2.

The respective vibrations from the top and the bottom explosive decks are easily identifiable in Figure 2. While the charge weights were approximately the same in the two decks, the persistent higher vibration levels due to the upper decks are attributed to the surface seismic waves and require further study.

A detailed study of blast-induced vibration can also be viewed in terms of peak particle velocity (PPV) vs. distance. Figures 3-a and 3-b show the distribution of PPVs corresponding to each deck

for the stations S1 and S2, respectively. Distances of the upper decks to the monitoring stations were approximately the same as the bottom decks. As stated before, PPV difference between the upper and bottom decks is related to the fact that the measured vibration from the upper deck was affected by the surface waves, while the recorded vibration from the bottom deck is governed primarily by the seismic 'body waves'. Results of this experiment also show how ground vibration from blasting, especially from bottom decks, may cause instabilities in the upper benches.

Figure 3.

Numerical Simulation

The Discrete Element Method (DEM) is based on the finite differences which can simulate a fractured medium as an assembly of rigid blocks. Discontinuities are represented as boundary conditions between rigid blocks and large displacements can be modeled along discontinuities (Jing and Stephansson, 2007). In 1979, Cundall and Strack proposed the Particle Discrete Element Method (P-DEM) as a novel implementation of the DEM method. A circular particle assemblage was used to model granular soils in this method. Later, its application was extended to the simulation of intact rock (Potyondy and Cundall, 2004). PFC2D and PFC3D which were developed by Itasca (Itasca, 2016) employ the Bonded Particle Method (BPM) to simulate intact rock (Potyondy and Cundall, 2004).

Bonded particle model has been used for the simulation of a single-hole blast, as well as in smooth blasting. In these models, gas expansion was also considered to model the whole blasting process (Potyondy et al., 1996, Yoon and Jeon, 2010). Resende et al. (2010) used PFC2D to study the compressive wave propagation through joints. Transmitted and reflected waves were compared to the theoretical solutions (Resende et al., 2010). However, the influence of vibration waves from blasting on the joint degradation has not been investigated in previous studies. This paper is focused on the effects of repetitive blasting on the degradation of a discrete joint in rock.

Sample Calibration

PFC simulates the rock as a dense packing of the non-uniform-sized circular rigid particles that are bonded together at their contact points. The bonds have their finite normal and shear stiffness. Relative particle motion is related to the force and moment at each contact by Newton's laws of motion. The advantage of the BPM is that unlike the continuum models, there is no need to use constitutive laws. Particle bonds behave under the applied load to the model, and can yield if the imposed levels of stress are higher than their strength. Bond breakage causes crack generation and development within the sample, which governs the mechanical behavior of the rock. Cracks are able to form, interact, and coalesce into macroscopic fractures according to local stress conditions.

The model requires that micro-mechanical properties be assigned to the particles and bonds in a way that result in representative intact rock properties. Potyondy and Cundall (2004) discussed the procedure of intact rock generation and calibration using bonded particle model. It involves particle size selection and matching the macro-properties of the rock sample. The numerical calibration is an iterative process which allows matching the macro-mechanical properties of the numerical model with the elastic modulus, Poisson ratio and uniaxial compressive strength of the rock sample.

The considered rock for this study is a massive sulfide rock with uniaxial compressive strength of 205MPa, elastic modulus of 104GPa, and Poisson ratio of 0.29. The rock sample is generated as a block of 2m×1m size with the minimum particle size of 1cm. The size of rock block was selected so that the numerical simulations could be performed in a reasonable computation time. Calibration procedure of the rock sample has been carried out to reach the similar macro

properties as the massive sulfide rock. Table I presents the micro-properties of the BPM rock sample. The resulting macro-properties of the BPM intact rock are shown in Table II which shows a good agreement with the intact rock properties of the massive sulfide rock.

Table I and Table II

Since the purpose of this study is the investigation of blast induced vibration effects on joint degradation, a single persistent joint was introduced in the rock sample. The joint thickness is 6cm which acts like a filled joint with an inclination angle of 45◦ from the horizontal. A smooth-joint contact model was used to simulate the mechanical properties of the joint (MasIvars et al. 2011, Itasca, 2016). The smooth-joint contact model allows the balls at the joint interface to overlap and slide past each other.

Similar to the intact rock, micro-properties of the smooth-joint should be calibrated during an iterative procedure. The jointed rock sample was tested by biaxial compression test with different confining pressures. Table III presents the calibrated micro-parameters of the smooth-joint. The obtained cohesion strength and friction angle of the persistent joint are 5.0 MPa and 31 degrees, respectively.

Table III

Boundary Conditions

For the investigation of ground vibration effect on the jointed rock in different benches, the longitudinal velocity component and vertical velocity component of the recorded vibrations in the stations S1 and S2 were selected, respectively. These two components were used because of their higher values compared to other components. These blast vibrations are not large enough to cause any damage to the intact part of the rock sample in S1 and S2 stations. However, the vibration energy may be sufficient to initiate and evolve damage within weak part of the rock (i.e. joint surface). The vibration histories were applied on the simulated jointed rock sample. In order to investigate the effect of repetitive blasting vibrations (i.e. multiple blasts) on the jointed rock sample, the same vibration histories were repetitively applied to the simulated jointed rock sample.

Figures 4-a and 4-c show the input histories for the stations S1 and S2, respectively. In addition, Figures 4-b and 4-d present the results of the Fast Fourier Transform of the ground vibrations at stations S1 and S2, respectively. The results show that the dominant wave frequency at the station S1 is approximately twice than that at station S2, as expected due to the latter's larger distance from the blast.

Figure 4

In this simulation, the blasting vibration was applied to the top of the rock sample (side A in Figure 5). A high damping value of 1.0 was assigned to the bottom of the model (side B) to absorb the energy of incoming waves. In order to absorb the vibration and prevent any reflection from the lateral sides of the rock sample, a quiet boundary has been considered for these sides of the rock sample (side C and D), where the displacement in these sides were fixed in the X-direction as can be observe in Figure 5. Since the objective of this study is the interaction of the blast induced vibration and joint, no damping was considered for the intact part of the rock.

Several virtual sensors, located above, within and below the joint plane, were used to monitor the velocity variation of the particles during the vibration event. In addition, virtual sensors close to the sample boundaries were employed to ensure that there is no significant reflection from the boundaries.

Figure 5.

Effects of Ground Vibration on Joint Degradation

Station S1

Figure 6 illustrates the cumulative damage to the jointed rock block model, after repeated application of the vibration loads presented in the Figure 4-a from detonation of single row of holes in the blast. It shows that the first blast (consisting of all 8 holes) led to generation of only 23 micro-cracks along the joint plane. The crack generation rate increased significantly during the subsequent vibration events. The maximum number of 1451 micro-cracks was reached within the joint zone at the end of the fifth blast. The cumulative number of cracks at the end of the fifth blast shows that most of the smooth-joint bonds yielded as the result of blasting vibrations. Consequently, the shear strength of the persistent joint is thus significantly reduced because of damage evolution due to these vibration events.

Figure 6

Station S2

The recorded ground vibration at station S2, shown in the Figure 4-c, was applied to the rock sample two consecutive times. Figure 7 shows the generation of micro-cracks within the joint zone as the result of blast induced vibration. The crack generation rate during the first blast was more than the generation rate in the case at station S1. It mainly related to the lower frequency of vibration for the station S2 vibration history. A total number of 1635 cracks was generated at the end of the second blast. The generated damaged zone within the joint zone at station S2 is found to be more extensive than the one generated at station S1.

Figure 7

Discussion

Cumulative damage in terms of the numbers of generated micro-cracks created along the joint surfaces versus the blasts for stations S1 and S2 are shown in Figure 8. Although, the particle velocity of the station S1 history was more than the station S2 history, the rate of crack generation along the joint surface in the case of S2 is much higher than the S1. The total number of micro-cracks generated during the five blasts, along the joint surface for station S1 (i.e. 1451), is lower than the generated cracks along the joint surface for station S2 (i.e. 1635). Due to impedance mismatch between the rock material and the joint zone, stress waves are reflected from upper and lower interfaces between the joint and the intact rock and thus, tensile stresses are applied on the joint filling material in the massive sulfide rock. The bonds along the joint surface are subjected to many loading and unloading cycles during each blast. Since the dominant frequency of blast waves from the S2 station is lower than the S1, the bonded infill material within the joint zone had enough time to react to the ground vibration and break. Therefore, more cracks/damage were generated during the first blast at location S2.

Conclusion

This paper dealt with the effects of double-deck blasting on the degradation of a persistent joint within a hard rock block. The recorded vibration history in a quarry was used as an input to the

numerical model. The bonded particle model was generated and calibrated based on the macro properties of a massive sulfide rock. Also, an inclined persistent joint was introduced to the rock sample. The recorded vibration particle velocity at the quarry was applied to the jointed rock sample. Virtual sensors around the joint plane and within the sample measured and recorded vibrations from the double-deck blasting.

The recorded ground vibration results showed that the recorded PPV corresponding to the upper decks were higher than those for the bottom decks. This is to be expected as the vibration amplitudes issuing from the upper explosive deck had a higher 'surface' wave content.

The cumulative crack number was measured during each blast. In the case of station S1, the results showed a slight increase in the number of cracks by the first blast, which is intensified by the subsequent blasts (total of five blasts). Crack generation rate in the case of station S2 on the upper bench was higher that the station S1. The lower frequency vibration history at S2 allowed the bonded infill material within the joint zone to have more time (between two consequent waves) to deform and fail due to the ground vibration. Therefore, a larger number of cracks were generated.

Numerical simulation results showed that the joint degradation rate in the case of ground vibrations with lower frequencies is much faster than the higher frequencies. It also provides a powerful tool in studying slope stability issues in response to very low but repeated vibration loads, although the vibration load from a single blast hole or a number of blast holes may be significantly below damage or instability threshold. This is particularly significant in view of large blasting operations involving hundreds of blast holes at a time, and repeated numerous times over the life of a mine.

Acknowledgement

The authors are grateful for the financial support provided by the National Science and Engineering Research Council of Canada (NSERC).

References

Blair, D.P. 2015. Wall control blasting. Proc. 11th Int. Symp. on Rock Fragmentation by Blasting (FRAGBLAST 11), Sydney, Australia, pp. 13-27.

Cundall, P.A., Strack, O.D.L. 1979. A discrete numerical model for granular assemblies. Geotechnique, vol:29, Issue 1, pp. 47-65.

Deb, D., Ryu, C.H., Kaushik, K.N.R., Jung, Y.B., Choi, B.H., Sunwoo, C. 2011. Stability assessment of a pit slope under blast loading: a case study of Pasir Coal Mine. Geotech. and Geol. Eng. vol: 29. pp. 419- 429.

Dianji, Z., Shiwei, B., Ping, T. 2002. The influence of vibratory stress on jointed rock Slope. 7th Int. Symp. on Rock Fragmentation by Blasting (FRAGBLAST 7), Beijing, China, pp. 755- 759.

Floyd, J.L. 1998. The development and implementation of efficient wall control blast design. Proc. 24th Ann. Conf. on Explosives and Blasting Tech., Florida, USA, pp. 77- 91.

Hu, Y., Yan, P., Lu, W., Yang, J., Chen, M. 2014. Comparison of blast-induced damage between presplit and smooth blasting of high rock slope. Rock Mech Rock Eng, vol: 47. pp. 1307- 1320

Itasca 2016. PFC2D - Two Dimensional Particle Flow Code, Ver. 5 User's Manual. Itasca Consulting Group, Minneapolis.

Jing, L., Stephansson, O. 2007. Fundamentals of discrete element methods for rock engineering. Elsevier. p.545.

Kong, W.K. 2012. Blasting assessment of slopes and risks planning. Australian. J. of Civil Eng, vol: 10. pp.177- 192.

Law, R., Keller, R. 1996. The stability of slopes subjected to blasting vibration

assessment and application in Hong Kong. Proc.12th Ann. Conf. on Explosives and Blasting Tech,, Florida, USA, pp. 47- 65.
Mohanty, B., Zwaan, D. 2015. Assessment of underground production blast design and blasting performance. Proc. 11th Int. Symp. on Rock Fragmentation by Blasting (FRAGBLAST 11), Sydney, Australia, pp. 607- 617.
Mohanty, B., Siamaki, A., Esmaieli, K. 2017. Effect of blasting vibrations from deck blasts on pit wall stability. Blasting and Fragmentation Journal. Vol: 11, Issue 1, pp. 37-47.
Naismith, W.A., Wessels, S.D.N. 2005. Management of a major slope failure at Nchanga Open Pit, Chingola, Zambia. J. South Africa Institute of Min. Met.; vol: 105. pp. 619–626.
O'Bryan, P. 2012. Wall failure and damage mechanisms. ACG-Australia Center for Geomechanics, Australia.
Onederra, I.A., Furtney, J.K., Sellers, E., Iverson, I. 2012. Modelling blast induced damage from a fully coupled explosive charge. Int. J. Rock Mech. Min. Sci.; vol: 58. pp. 73- 84.
Potyondy, D.O., Cundall, P.A., Sarracino, R.S. 1996. Modeling of shock and gas driven fractures induced by a blast using bonded assemblies of spherical particles. Proc.5th Int. Symp. on Rock Fragmentation by Blasting (FRAGBLAST 5); Canada, pp. 55- 62.
Potyondy, D., Cundall, P.A. 2004. A bonded particle model for roc; Int. J. Rock Mech. Min. Sci, vol:41. pp. 1329- 1364.
Resende, R., Lamas, L.N., Lemos, J.V., Calcada, R. 2010. Micromechanical modelling of stress waves in rock and rock fractures. Rock Mech Rock Eng, vol: 43. pp. 741- 761.
Resende, R., Fortunato, E., Andrade, C., Miranda, T. 2014. Vibration propagation in discrete element particle models of rock; EUROCK2014: Structures in and on Rock Masses, pp. 871- 876.
Yang, R., Wittaker, T., Kirkpatrick, S. 2009. PPV Measurement and frequency shifting in soft ground near highwalls to reduce blast damage. Proc. 35th Ann. Conf. on Explosives and Blasting Tech. Florida, USA.
Yoon, J., Jeon, S. 2010. Use of a modified particle-based method in simulating blast-induced rock fracture; Proc. 9th Int. Symp. on Rock Fragmentation by Blasting (FRAGBLAST 9), Spain, pp. 371- 380.

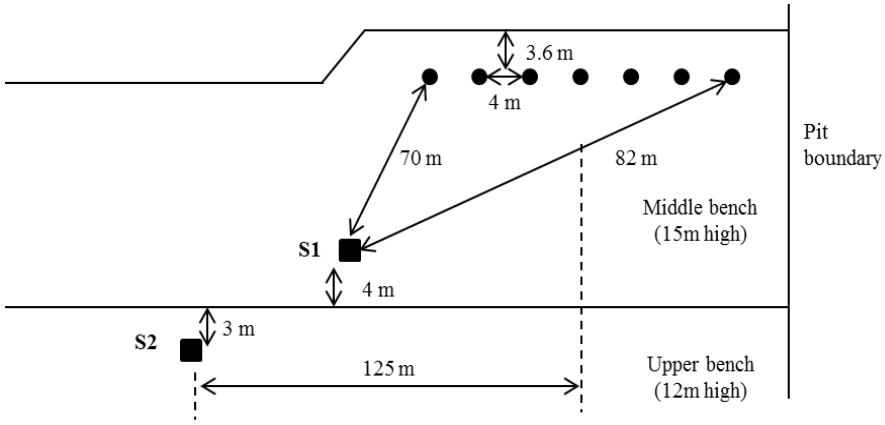

S1 , S2 : Seismic Stations

Figure 1- Schematic view of blast areas and recording stations

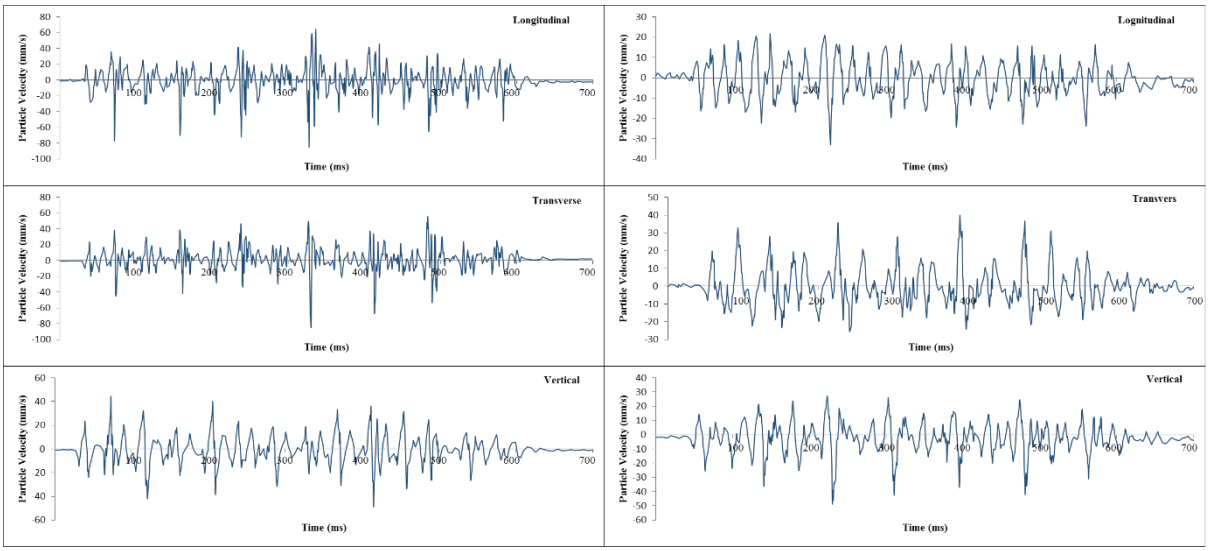

a- Station S1 b- Station S2

Figure 2- Recorded blast vibration from the single row blast in the a- Station S1 and b- Station S2

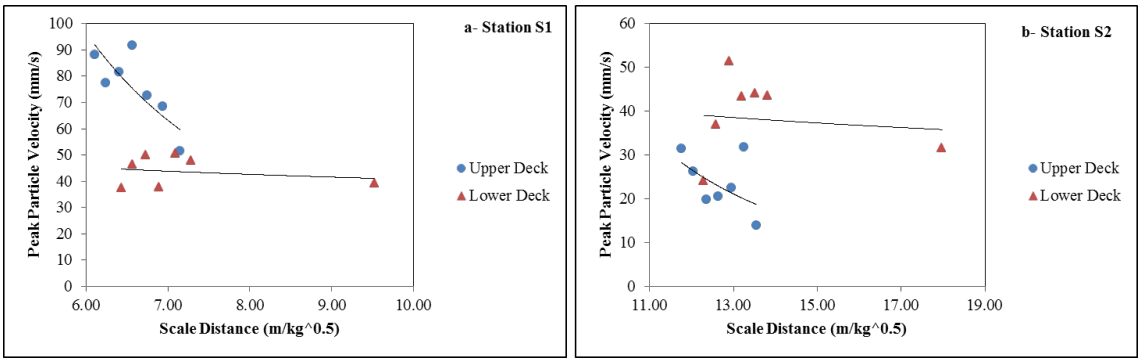

Figure 3- Peak particle velocity vs. scale distance for: a- Station S1, b- Station S2

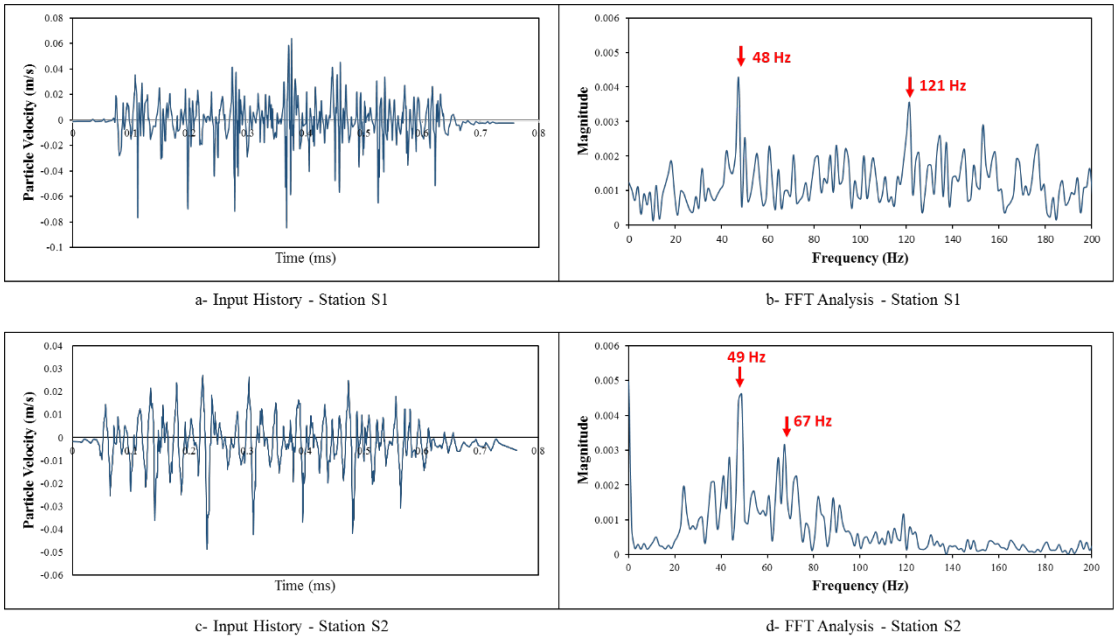

Figure 4- Input ground vibration history to the numerical model, a- station S1 history, b- station S1 FFT analysis results, c- station S2 history, d- station S2 FFT analysis results

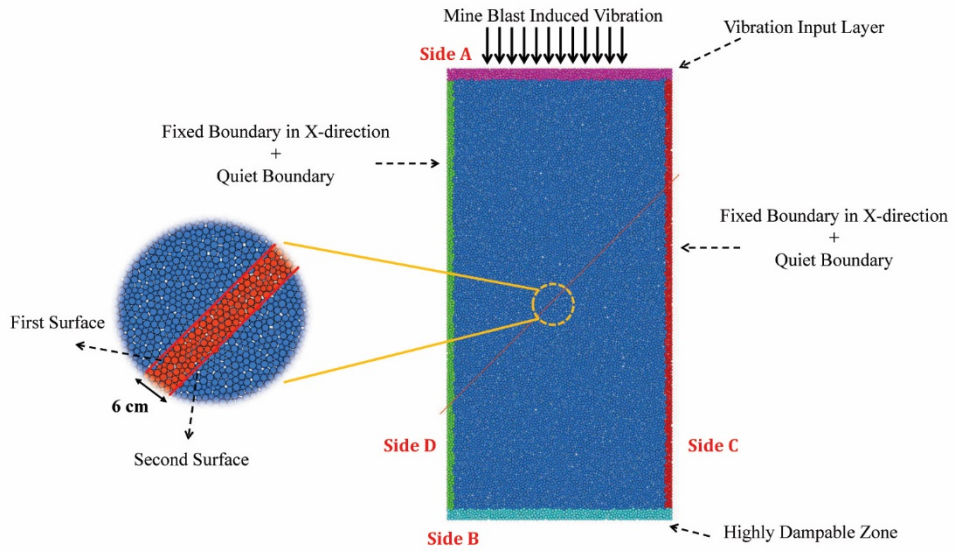

Figure 5- Boundary conditions of the numerical rock sample: the vibration load is applied from the side A, the Quiet boundary as the absorbing boundary was assigned to the sides C and D and a highly damping factor was considered for the side B. The joint zone thickness is also shown as 6 cm.

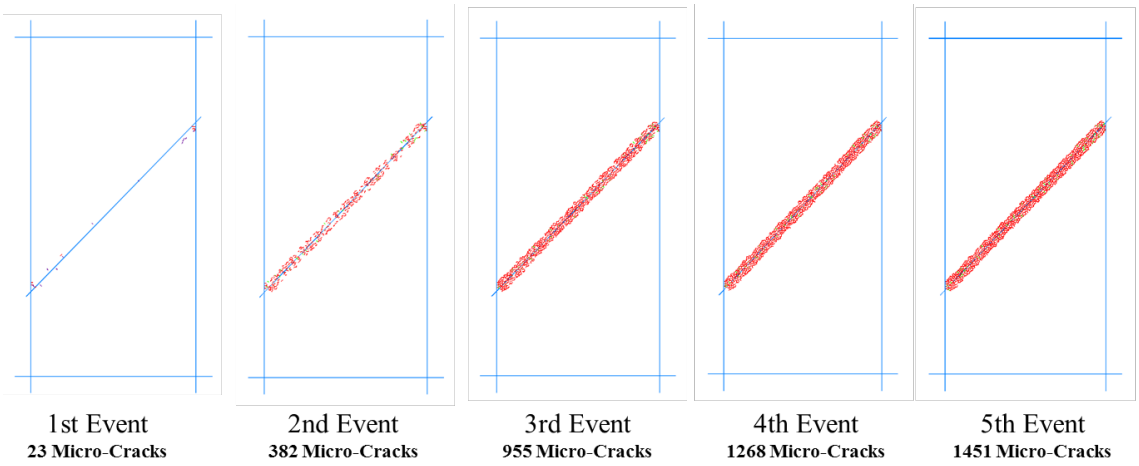

Figure 6- Damage accumulation in the jointed rock block sample due to repeated vibration loading from five consecutive blasts (corrresponding to respective vibration loads ftom station S1).

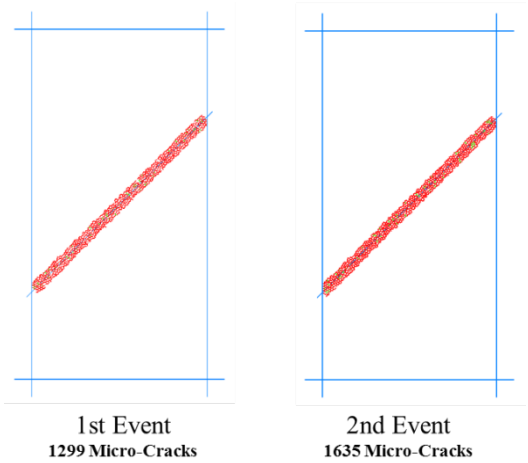

Figure 7- Damage accumulation in the jointed rock block sample due to repeated vibration loading from two concequtive blasts (corrresponding to respective vibration loads ftom station S2).

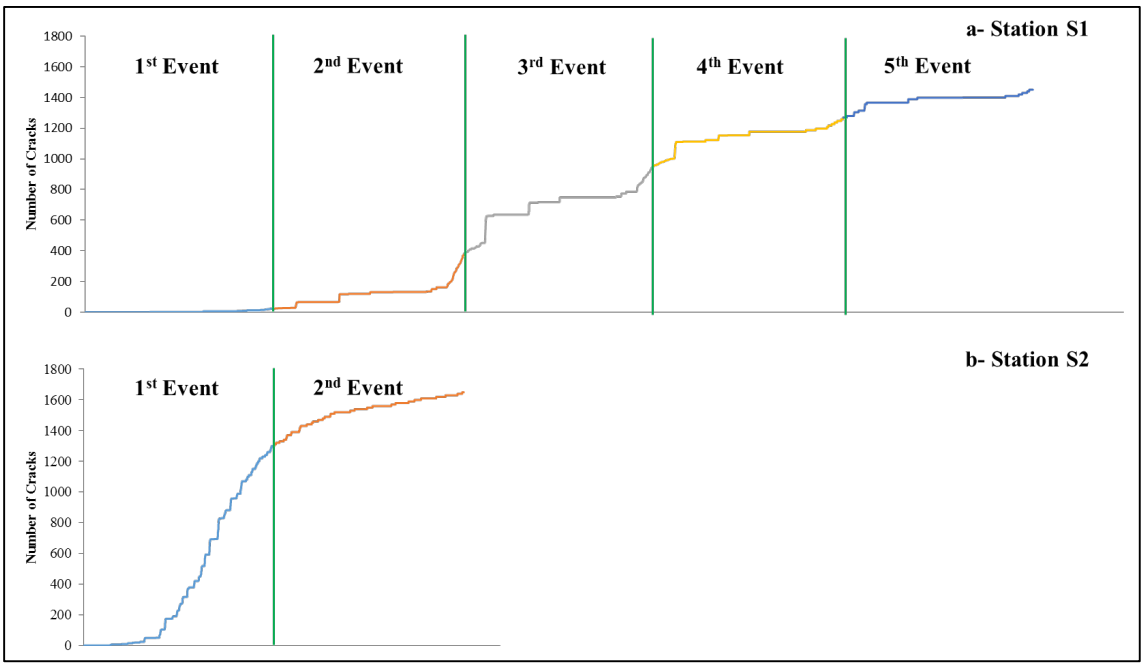

Figure **8-** Number of generated cracks during each blast for the station S1 and station S2

Table I- Micro mechanical properties of the calibrated BPM rock sample

Properties	Value
Elastic Modulus (GPa)	50
Stiffness Ratio (Normal /Shear Stiffness)	2.5
Tensile Strength (MPa)	55
Cohesion Strength (MPa)	55
Friction Value	0.577

Table II- Mechanical properties of the massive sulfide rock and the calibrated bonded particle model

Mechanical properties	Massive sulfide rock	PFC2D
Elastic Modulus (GPa)	104	104
Uniaxial Strength (MPa)	205	202
Poisson's Ratio	0.29	0.27
Density (gr/cm^3)	4.3	4.3

Table III- Micro-parameters of the calibrated smooth-joint

Properties	Value
Normal Stiffness (GPa)	20
Shear Stiffness (GPa)	10
Friction Coefficient	0.577
Cohesion Strength (MPa)	0.8
Tensile Strength (MPa)	0.8